nature biotechnology

Massively parallel polymerase cloning and genome sequencing of single cells using nanoliter microwells

Jeff Gole[1], Athurva Gore[1], Andrew Richards[1], Yu-Jui Chiu[2], Ho-Lim Fung[1], Diane Bushman[3], Hsin-I Chiang[1,5], Jerold Chun[3], Yu-Hwa Lo[4] & Kun Zhang[1]

Genome sequencing of single cells has a variety of applications, including characterizing difficult-to-culture microorganisms and identifying somatic mutations in single cells from mammalian tissues. A major hurdle in this process is the bias in amplifying the genetic material from a single cell, a procedure known as polymerase cloning. Here we describe the microwell displacement amplification system (MIDAS), a massively parallel polymerase cloning method in which single cells are randomly distributed into hundreds to thousands of nanoliter wells and their genetic material is simultaneously amplified for shotgun sequencing. MIDAS reduces amplification bias because polymerase cloning occurs in physically separated, nanoliter-scale reactors, facilitating the *de novo* assembly of near-complete microbial genomes from single *Escherichia coli* cells. In addition, MIDAS allowed us to detect single-copy number changes in primary human adult neurons at 1- to 2-Mb resolution. MIDAS can potentially further the characterization of genomic diversity in many heterogeneous cell populations.

The genetic material in a single cell can be amplified *in vitro* by DNA polymerase into many clonal copies, which can then be characterized by shotgun sequencing. Single-cell genome sequencing has been successfully demonstrated on microbial and mammalian cells[1–6] and applied to the characterization of the diversity of microbial genomes in the ocean[7], somatic mutations in cancers[8,9], and meiotic recombination and mutation in sperm[3,10]. The most commonly used method for amplifying DNA from single cells is multiple displacement amplification (MDA)[2]. The major technical challenge in using MDA is the highly uneven amplification of the one or two copies of each chromosome in a single cell. This high amplification bias leads to difficulties in assembling microbial genomes *de novo* and inaccurate identification of copy number variants (CNV) or heterozygous single-nucleotide changes in single mammalian cells. Recently developed bias-tolerant algorithms[11,12] have greatly mitigated the effects of uneven read depth on *de novo* genome assembly and CNV calling, yet either unusually high sequencing depth or relatively low-resolution analysis is required.

Several strategies have been developed to reduce amplification bias, including reducing the reaction volume[13,14] and supplementing amplification reactions with single-strand binding proteins or trehalose[5,15]. Post-amplification normalization by digesting highly abundant sequences with a duplex-specific nuclease has also been used to markedly reduce bias[2]. Despite these efforts, amplification bias remains the biggest challenge in single-cell genome sequencing. A relatively large amount of sequencing is still necessary to obtain a high-quality genome sequence even with these improvements. Using cells that contain multiple copies of the genome or multiple clonal cells has been the only viable solution to achieve near-complete genome coverage with MDA[16,17]. Other methods such as MALBAC utilize quasi-linear amplification to reduce exponential amplification bias[18]; however, the specific polymerase required can introduce more amplification errors, complicating further analysis.

We reasoned that whole-genome amplification is always prone to bias because repeated priming in similar locations becomes exponentially more favorable as the reaction continues. Thus, we hypothesized that bias could be reduced by limiting the reaction so that just enough amplification occurs to allow sequencing, thereby limiting the potential iterations of repeated priming. In addition, we supposed that reducing the reaction volume by ~1,000-fold to nanoliter levels, which increases the effective concentration of the template genome, might both reduce contamination and improve amplification uniformity, as the higher concentration of template would lead to more favorable primer-annealing kinetics in the initial stages of MDA[13,14].

To test these hypotheses, we developed MIDAS, an approach that allows for highly parallel polymerase cloning of single cells in thousands of nanoliter reactors. Each reactor spatially confines a reaction within a 12-nl volume, to our knowledge the smallest volume that has been implemented to date. Coupled with a low-input library construction method, we achieved highly uniform coverage in the genomes of both microbial and mammalian cells. We demonstrated substantial improvement both in *de novo* genome assembly from single microbial cells and in the ability to detect small somatic CNVs in individual human adult neurons with minimal sequencing effort.

[1]Department of Bioengineering, Institute for Genomic Medicine and Institute of Engineering in Medicine, University of California at San Diego, La Jolla, California, USA. [2]Materials Science and Engineering Program, University of California at San Diego, La Jolla, California, USA. [3]Dorris Neuroscience Center, Department of Molecular and Cellular Neuroscience, The Scripps Research Institute, La Jolla, California, USA. [4]Department of Electrical and Computer Engineering, University of California at San Diego, La Jolla, California, USA. [5]Present address: Department of Animal Science, National Chung Hsing University, Taichung, Taiwan. Correspondence should be addressed to K.Z. (kzhang@bioeng.ucsd.edu).

Received 23 April; accepted 13 September; published online 10 November 2013; doi:10.1038/nbt.2720

RESULTS

MIDAS implements massively parallel polymerase cloning

We designed and fabricated microwell arrays of a size comparable to standard microscope slides. The format of the arrays, including well size, pattern and spacing, was optimized to achieve efficient cell loading, optimal amplification yield and convenient DNA extraction. Each slide consisted of 16 arrays, each containing 255 microwells 400 µm in diameter, allowing for parallel amplification of 16 separate heterogeneous cell populations (**Fig. 1a**). All liquid handling procedures (cell seeding, lysis, DNA denaturation, neutralization and addition of amplification master mix) required one pump of a pipette per step per array, minimizing the labor required for hundreds of amplification reactions. This system requires less of each amplification and library construction reagent than conventional methods, as each microwell spatially confines the reaction to 12 nl.

We tested multiple cell-loading densities to ensure that each well would contain only one single cell, and we initially loaded the microwells at densities of roughly one cell per well and one cell per ten wells. By the Poisson distribution, in the one cell per well case, 63% should have at least one cell, but 26% could have more than one. In the one cell per ten well case, no more than 0.5% of the wells should contain more than one cell. We confirmed that the cells were indeed being seeded at the expected distribution using fluorescent microscopy after staining cells with SYBR Green I (**Supplementary Fig. 1**). We thus decided to load cells at a density of one cell per ten wells, ensuring that 99.5% of generated amplicons would arise from a single cell. The remaining empty wells served as internal negative controls, allowing easy detection and elimination of contaminated samples. We further confirmed proper microbial and mammalian cell seeding in microwells at the one-cell-per-ten-well level by scanning electron microscopy (**Fig. 1b** and **Supplementary Fig. 2**).

After seeding cell populations into each microwell array, we performed limited MDA on the seeded single cells in the partitioned microwells, each with a physically separated (save for a thin aqueous layer atop the arrays) volume of ~12 nl, in a temperature- and humidity-controlled chamber (**Fig. 1c** and **Supplementary Fig. 1**). We used SYBR Green I to visualize the amplicons growing using an epifluorescent microscope (**Supplementary Fig. 3**). A random distribution of amplicons across the arrays was observed with ~10% of the wells containing amplicons, further confirming the parallel and localized amplification within individual microwells as well as the stochastic seeding of single cells[19]. After amplification in the microwells, we used a micromanipulation system to extract amplicons from individual wells for sequencing (**Fig. 1c**). We estimated that the masses of the extracted amplicons ranged from 500 pg to 3 ng.

When performing a single-cell amplification experiment, there are two potential sources of contamination that could result in an inaccurate characterization of the genome of the sample of interest. These are exogenous contamination, in which samples are exposed to cell-free DNA from environmental sources or reagents, and cross-well contamination, in which DNA from one microwell diffuses into other microwells. We ensured that neither form of contamination was occurring. To detect arrays that contained exogenous contamination, we checked for a uniform increase of fluorescent signal across all microwells. Any samples that showed this high fluorescence across all wells were removed; thus, any samples exposed to cell-free DNA were simply not analyzed. To ensure that cross-well contamination was not occurring, we performed fluorescent monitoring at 30-min intervals during the amplification procedure. Only single wells with single amplicons originating from a single point were extracted for analysis, preventing any cross-well contamination or selection of any wells containing more than one cell (**Supplementary Fig. 4**). If even a miniscule amount of DNA was diffusing out of a microwell, an increased fluorescence would be observed in adjacent wells owing to amplification occurring in every well[19]; this diffusion was not observed in any microwells. We further confirmed that cross-well contamination was not occurring by loading a mixture of human neuronal nuclei with two separate genomic backgrounds and confirming that all extracted cells corresponded only to one background (**Supplementary Table 1**).

To construct Illumina sequencing libraries from the extracted nanogram-scale DNA amplicons, we used a modified in-tube method based on the Nextera Tn5 transposase. Previous studies have shown that Nextera transposase-based libraries can be prepared using as little as 10 pg of genomic DNA[20]. However, the standard Nextera protocol was unable to generate high-complexity libraries from MDA

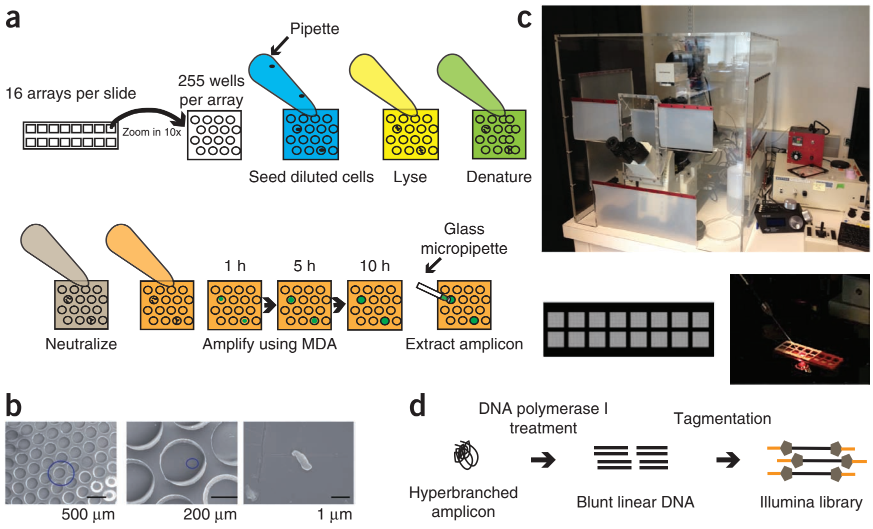

Figure 1 MIDAS. (**a**) Each slide contains 16 arrays of 255 microwells each. Cells, lysis solution, denaturing buffer, neutralization buffer and MDA master mix were each added to the microwells with a single pipette pump. Amplicon growth was then visualized with a fluorescent microscope using a real-time MDA system. Microwells showing increasing fluorescence over time were positive amplicons. The amplicons were extracted with fine glass pipettes attached to a micromanipulation system. (**b**) Scanning electron microscopy of a single *E. coli* cell displayed at different magnifications. This particular well contains only one cell, and most wells observed also contained no more than one cell. (**c**) A custom microscope incubation chamber was used for real time MDA. The chamber was temperature and humidity controlled to mitigate evaporation of reagents. Additionally, it prevented contamination during amplicon extraction because the micromanipulation system was self-contained. An image of the entire microwell array is also shown, as well as a micropipette probing a well. (**d**) Complex three-dimensional MDA amplicons were reduced to linear DNA using DNA polymerase I and Ampligase. This process substantially improved the complexity of the library during sequencing.

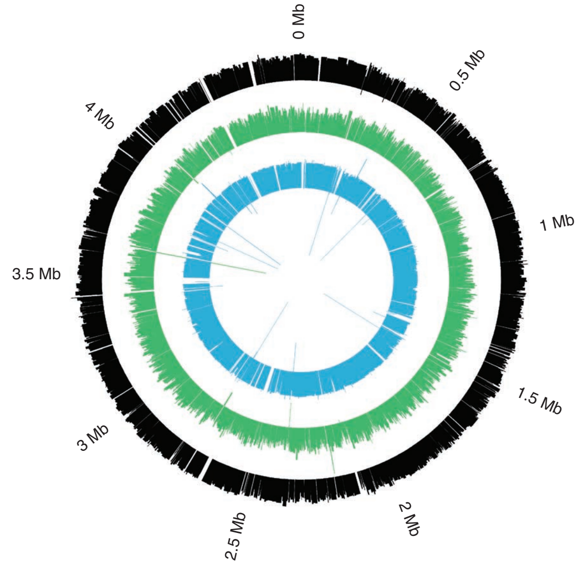

Figure 2 Depth of coverage of assembled contigs aligned to the reference *E. coli* genome. Three single *E. coli* cells were analyzed using MIDAS. Between 88% and 94% of the genome was assembled from 2–8 million paired-end 100-bp reads. Each colored circle is a histogram of the $\log_2$ of average depth of coverage across each assembled contig for one cell. Gaps are represented by blank whitespace in between colored contigs.

amplicons, resulting in poor genomic coverage (data not shown). To address this issue, we used random hexamers and DNA polymerase I to first convert the hyperbranched amplicons into unbranched double-stranded DNA molecules, which allowed effective library construction using *in vitro* transposition (**Fig. 1d**). In addition, we used a small reaction volume to further increase the efficiency of library construction[20].

Generation of a near-complete assembly from single *E. coli*

As a proof-of-concept experiment, we used MIDAS to sequence three single MG1655 *E. coli* cells, generating 2- to 8-million paired-end Illumina MiSeq sequencing reads of 100 bp in length for each cell, which is equivalent to a genomic coverage of 87–364×. We first mapped the reads to the reference *E. coli* genome and recovered 98–99% of the genome at >1× coverage. Even when reads were down-sampled such that genomic sequencing coverage was much lower (10×), we still recovered a high percentage of the genome (90%) (**Supplementary Fig. 5**). We then assembled the genome *de novo* using SPAdes[11]. We assembled 88–94% of the *E. coli* genome (**Fig. 2**), with an N50 contig size (i.e., the size at which all longer contigs represent half of the assembled sequence) of 2,654–27,882 bp and a maximum contig length of 18,465–132,037 bp. More than 80% of the assembled bases were mapped to *E. coli*, with the remainder resulting from common MDA contaminants such as *Delftia* and *Acidovorax* (**Supplementary Fig. 6** and **Supplementary Table 2**). Despite the higher initial template concentration in the MIDAS libraries, chimerism was present at a comparable level to that previously reported for Illumina sequencing libraries constructed from conventional in-tube MDA reactions, with 1 chimeric junction per ~5 kb[2] (**Supplementary Table 3**). We annotated the genome using the RAST and KAAS annotation servers. Over 96% of *E. coli* genes was either partially or fully covered in the assembly. Major biosynthetic pathways, including glycolysis and the citric acid cycle, were also present. Furthermore, pathways for amino acid synthesis and tRNA development were covered. MIDAS was thus able to assemble an extremely large portion of the *E. coli* genome from a single cell with comparatively minimal sequencing.

As a control, we also amplified and sequenced one *E. coli* cell using the conventional in-tube MDA method[1], and controlled the reaction time to limit the amplification yield to the nanogram level. A fraction of the control amplicon was further amplified in a second reaction to the microgram level. The two control amplicons were converted into sequencing libraries using the conventional shearing and ligation method. We found that limiting the amplification yield reduced amplification bias, even for in-tube amplification. However, MIDAS had a markedly reduced level of amplification bias when compared with either control reaction (**Fig. 3a**,**b**). MIDAS was also able to recover a much larger fraction of the genome than the conventional MDA-based method. In fact, when compared with the most complete previously published single *E. coli* genome data set[7], MIDAS recovered 50% more of the *E. coli* genome with 3- to 13-fold less sequencing data (~90–400× versus ~1,200×). This result demonstrates that MIDAS provides a much more efficient way to assemble whole bacterial genomes from single cells without culture.

Identification of CNVs in single neurons

We next applied MIDAS to the characterization of CNVs in single mammalian cells. The high cognitive function of the human brain is supported by a complex network of neurons and glia. It has long been thought that all cells in a human brain share the same genome. Recent evidence suggests that individual neurons could have nonidentical genomes owing to aneuploidy[21–24], active retrotransposons[25,26] and other DNA content variation[27].

To demonstrate the viability of MIDAS as a tool for investigating CNVs in single primary human neurons, we prepared nuclei from one post-mortem brain sample from a disease-free female and a second post-mortem brain sample from a female with Down syndrome. We purified cortical neuronal nuclei by flow sorting based on neuron-specific NeuN antibody staining. We generated six sequencing libraries (two disease-free and four Down syndrome) from individual nuclei using MIDAS and analyzed the data using a method based on circular binary segmentation to call CNVs[28] (**Supplementary Table 4**). Raw sequencing reads were divided into 49,891 genomic bins ~60 kb in size, each of which had been previously determined to contain a similar number of sequencing reads in a fully diploid cell[28]. Although clonal read counts arising from PCR duplication appeared relatively high, this is a consequence of the low-input Nextera library construction protocol; because the amplification is limited, the number of initial molecules is smaller, leading to more duplicates. However, the reduction in bias compensated for the apparent decrease in usable read count. We similarly observed a marked reduction of amplification bias in the MIDAS libraries when compared to the conventional in-tube, MDA-based method (**Fig. 3c**,**d**). However, both MIDAS and in-tube MDA had higher levels of sequencing bias and variability than data generated from unamplified genomic DNA from 4,000 mammalian cells, though the bias in MIDAS was only slightly higher. Using a larger bin size of ~240 kb (which results in a lower-resolution analysis) allowed MIDAS to match the level of bias from unamplified genomic DNA (**Supplementary Fig. 7**).

We next sought to characterize the sensitivity of detecting single copy-number changes. It was not possible to distinguish true copy-number differences from random amplification bias for the conventional single-cell MDA data, even with aggressive binning into large genomic regions. However, the uniform genome coverage in the MIDAS libraries allowed clear detection of trisomy 21 in each of the Down syndrome nuclei (**Fig. 4a**,**b**). Rigorous validation

Figure 3 Genomic coverage of single cells amplified by MDA in a tube and by MIDAS. The observed multipeak profile for the MDA reactions implies that certain regions may have been amplified with exponentially greater bias compared to the majority of the genome. (**a**) Comparison of single *E. coli* cells amplified in a PCR tube for 10 h (top), 2 h (middle) and in a microwell (MIDAS) for 10 h (bottom). Genomic positions were consolidated into 1-kb bins (*x* axis), and were plotted against the $\log_{10}$ ratio (*y* axis) of genomic coverage (normalized to the mean). (**b**) Distribution of coverage of amplified single bacterial cells. The *x* axis shows the $\log_{10}$ ratio of genomic coverage normalized to the mean. (**c**) Comparison of single human cells amplified using traditional MDA in a PCR tube for 10 h (top) or in a microwell (MIDAS) for 10 h (middle) to a pool of unamplified human cells (bottom). Genomic positions were consolidated into variable bins of ~60 kb in size, previously determined to contain a similar read count[28], and were plotted against the $\log_{10}$ ratio (*y* axis) of genomic coverage (normalized to the mean). (**d**) Distribution of coverage of amplified single mammalian cells. The *x* axis shows the $\log_{10}$ ratio of genomic coverage normalized to the mean.

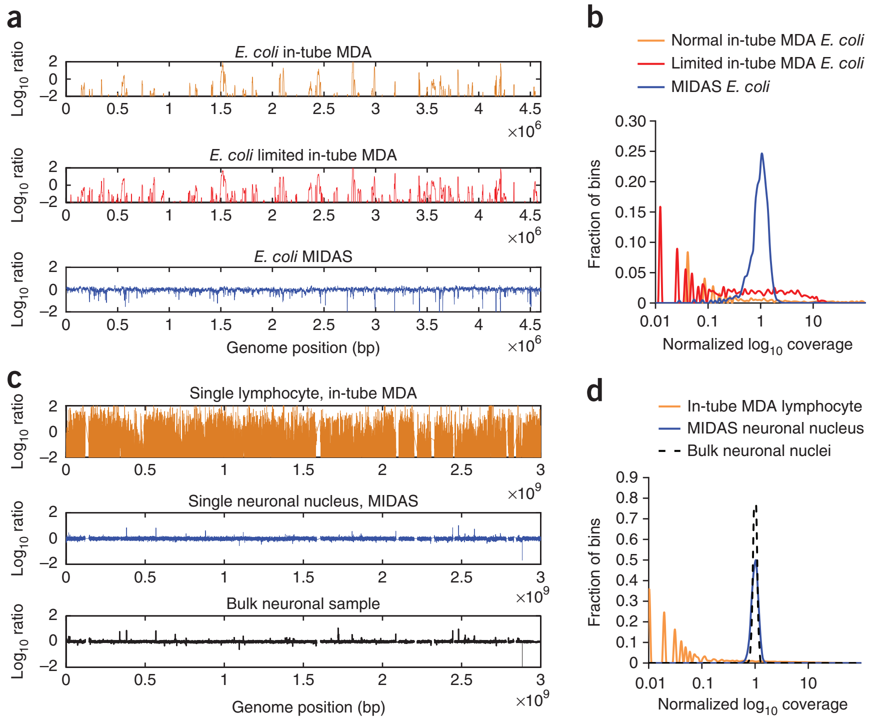

of single-cell sequencing methods has been extremely challenging, primarily because any single cell might have genomic differences that are not detectable in the bulk cell population. Hence, there is no reference genome that single-cell data can be compared to. To determine the CNV detection limit of MIDAS, we computationally simulated sequencing data sets containing reference CNV events 1 or 2 Mb in size. We randomly selected 1- or 2-Mbp regions of either chromosome 21 (to simulate the gain of a single copy, the smallest possible copy number change) or chromosome 4 (as a negative control), and computationally transplanted these regions into 100 other random genomic locations (**Supplementary Table 5**). This computational approach, similar to a strategy previously used for assessing sequencing errors[29], yielded data sets containing reference CNVs at known positions without affecting the inherent technical noise in the data. We identified 99/100 2-Mb T21 insertions and 80/100 of 1-Mb T21 insertions in the simulated data set from Down syndrome cell 1, indicating that MIDAS is able to call copy number events at the megabase-scale with high sensitivity (**Fig. 4c** and **Supplementary Table 5**). As expected, detection levels in the other data sets were similar for libraries with sufficient sequencing depth (80/100 for Down syndrome cell 2, 99/100 for Down syndrome cell 4), whereas libraries with insufficient sequencing depth could not be used for calling small CNVs accurately (32/100 for Down syndrome cell 3). As expected, the insertion of diploid chromosome 4 regions did not generate any copy number calls. High-fidelity CNV calling (96%) at the 2-Mb level was retained even when 20% additional random

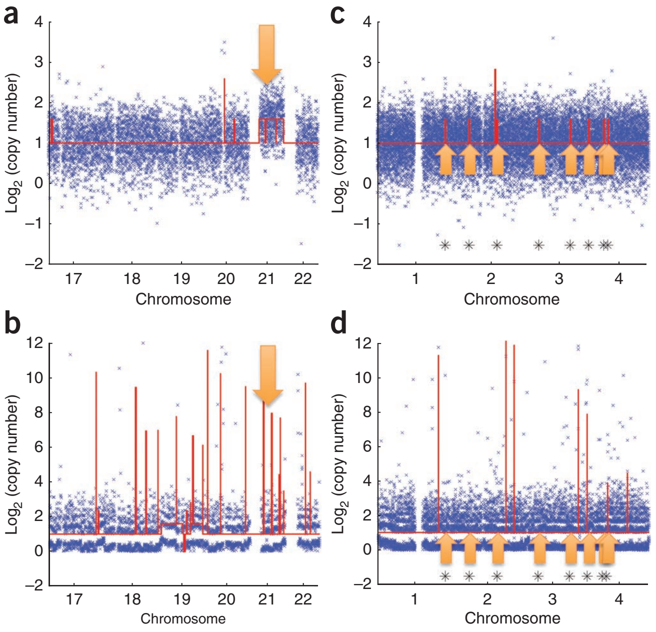

Figure 4 Detection of CNVs. Genomic positions were consolidated into bins of ~60 kb in size which were previously determined to contain a similar read count[28]. Estimated copy numbers below were rounded to the nearest whole number. (**a**) CNVs in a Down syndrome single cell analyzed with MIDAS. The *x* axis shows genomic position. The *y* axis shows (on a $\log_2$ scale) the estimated copy number as a red line. The arrow indicates trisomy 21, which is clearly visible in this single cell. (**b**) CNVs in a Down syndrome single cell analyzed with traditional in-tube MDA. The *x* axis shows genomic position. The *y* axis shows (on a $\log_2$ scale) the estimated copy number as a red line. The arrow marks the expected region of trisomy 21, which is not detectable in these data. (**c**) CNVs in a Down syndrome single cell with trisomy 21 'spike-ins'. The *x* axis shows genomic position. The *y* axis shows (on a $\log_2$ scale) the estimated copy number as a red line. At each arrow, before CNV calling, data from a randomly determined 2 Mb section of trisomy chromosome 21 were computationally inserted into the genome, simulating a small gain-of-single-copy event. At each location, a CNV was called, showing that MIDAS can detect 2-Mb CNV accurately. (**d**) CNV in a Down syndrome single cell with trisomy 21 spike-ins. The *x* axis shows genomic position. The *y* axis shows (on a $\log_2$ scale) the estimated copy number as a red line. At each arrow, before CNV calling, data from a randomly determined 2 Mb section of trisomy chromosome 21 was computationally inserted into the genome, simulating a small gain-of-single-copy event.

technical noise was applied to the read count results (**Supplementary Fig. 8**). When the same simulation was done with data from traditional in-tube MDA libraries, no T21 insertions were detected, indicating that at this sequencing depth, traditional MDA-based methods were unable to call small CNVs (**Fig. 4d**).

We next performed CNV calling on each individual neuron using the parameters calibrated by the T21 transplantation simulation. MIDAS called 9–18 copy number events in each neuron (**Supplementary Table 6**). Only 8/60 called CNV events were >2 Mb, and only 13/60 were >1 Mb. It remained unclear whether the remaining events represented true copy number changes or whether they were false positives owing to the small size of most of the calls. It was also unclear which CNV calls represented somatic CNVs and which represented germline CNV calls that might have been missed in one sample. To address these issues and further probe the ability of MIDAS to identify germline and *de novo* CNV events, we performed library construction and sequencing on unamplified genomic DNA from two pools of ~4,000 neuronal nuclei from the healthy donor, and compared the results to those obtained from the same donor's single neuronal nuclei (**Supplementary Table 7**). We identified 22 CNV events in the unamplified libraries, of which only two were not shared between the two pools; these are likely false-positive or false-negative CNV calls in one sample. However, no CNV events identified in the pools were >1 Mb. This finding is not surprising, as germline CNV events >1 Mb do not commonly occur[30]. Although MIDAS does not have sufficient specificity when calling CNVs <1 Mb, we investigated how much small germline CNVs could be identified in the single-cell libraries, and found that 75% were detected. Overall, based on the T21 computational transplantation results, it appears that the five individual human neurons (excluding Down syndrome cell 3 owing to insufficient sequencing depth) contain an average of one region each with a somatic gain of one copy at the megabase scale, and that several smaller CNV events might also be present.

DISCUSSION

Owing to the extreme bias caused by whole-genome amplification from a single DNA molecule, genomic analysis of single cells has remained a challenging task. A great deal of sequencing resources is required to produce a draft-quality genome assembly or determine a low-resolution CNV profile owing to amplification bias and coverage dropout. MIDAS addresses this issue through the use of nanoliter-scale spatially confined volumes to generate nanogram-scale amplicons and the use of a low-input, transposon-based, library construction method. Compared to the conventional single-cell library construction and sequencing protocol, MIDAS provides a more uniform, higher-coverage approach to analyze single cells from a heterogeneous population (**Supplementary Table 8**).

We applied MIDAS to single *E. coli* cells and resolved nearly the entire genome with relatively low sequencing depth. Additionally, using *de novo* assembly, >90% of the genome was assembled with far less sequencing effort than in traditional MDA-based methods. These results suggest that applying MIDAS to an uncultivated organism would provide a draft quality assembly. Currently, a majority of unculturable bacteria are analyzed using metagenomics, as part of a mixed population rather than individually. Metagenomics has only recently allowed for the assembly of genomes from single cells, and doing so requires a sample with limited strain heterogeneity[31]. Through the use of MIDAS on heterogeneous environmental samples, novel single-cell organisms and genes can be easily discovered and characterized in a high-throughput manner, allowing a much higher resolution and more complete analysis of single microbial cells.

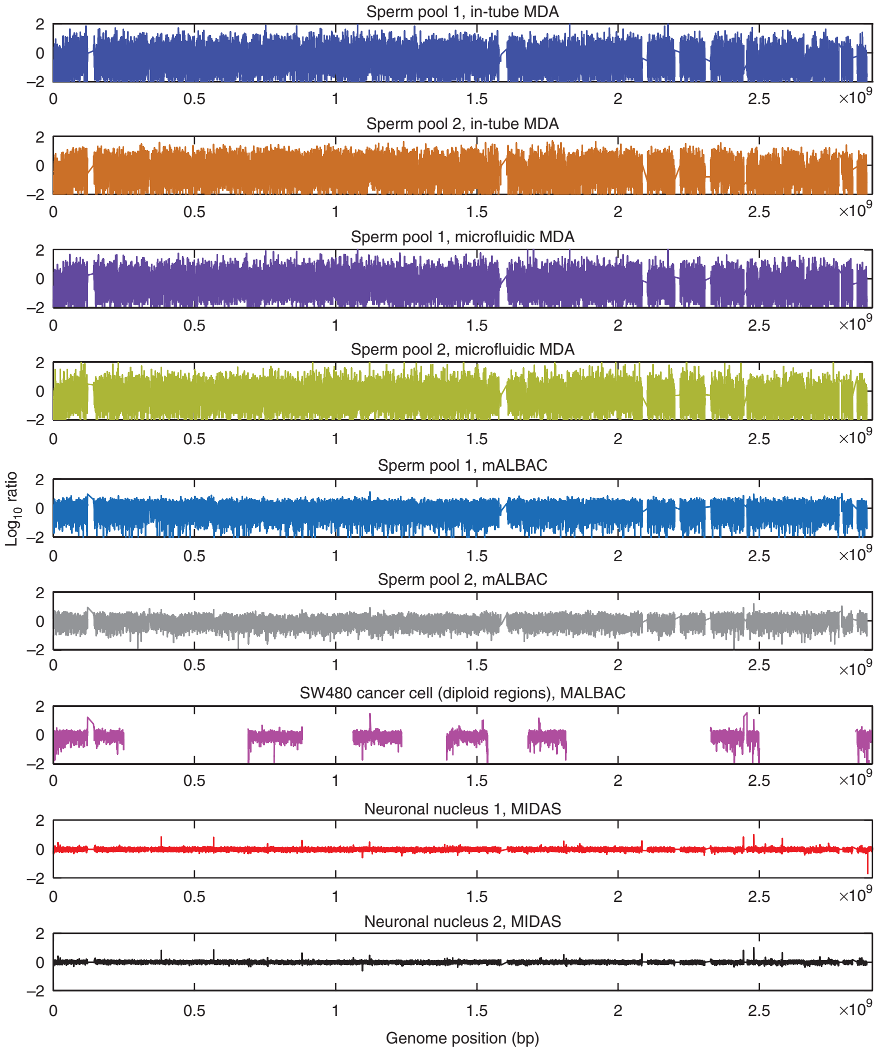

Figure 5 Comparison of MIDAS to previously published data for in-tube MDA[32], microfluidic MDA[10] and MALBAC[33] for diploid regions of pools of two sperm cells and diploid regions of a single SW480 cancer cell processed using MALBAC[18]. Genomic positions were consolidated into variable bins of ~60 kb in size previously determined to contain a similar read count[28] and were plotted against the $\log_{10}$ ratio (*y* axis) of genomic coverage (normalized to the mean). For the cancer cell data, nondiploid regions have been masked out (white gaps between pink) to remove the bias generated by comparing a highly aneuploid cell to a primarily diploid cell.

We also applied MIDAS to the analysis of CNVs in single human neuronal nuclei. With <0.4× coverage, we used MIDAS to call single copy number changes of 1–2 million base pairs or larger in size. It has been shown recently that, in human adult brains, post-mitotic neurons in different brain regions exhibit various levels of DNA content variation[27]. The exact genomic regions that are associated with DNA content variation has been difficult to map to single neurons because of the amplification bias with existing MDA-based methods. CNVs in single tumor cells have been successfully characterized with a PCR-based, whole-genome amplification method[8]. However, tumor cells tend to be highly aneuploid and exhibit copy number changes of larger magnitude, which are more easily detected. The applicability of a PCR-based strategy to other primary cell types with more subtle CNV events remains unclear. We have demonstrated that MIDAS greatly reduces the variability of single-cell analysis to a level such that a 1- to 2-Mb, single-copy change is detectable, allowing characterization of much more subtle CNVs. With additional improvements in sequencing methods, the use of MIDAS might enable the identification of even smaller CNVs, as currently 75% of smaller germline CNVs below the recommended detection limit of MIDAS are still identifiable in single cells. Thirteen somatic gain-of-single-copy events at the megabase level were identified in single neurons, and it appeared that several protease inhibitors, genes involved in vesicle formation and genes involved in coagulation could be affected (**Supplementary Table** 7). A majority of gene copy changes occurred in one single cell, indicating that gene copy number might greatly vary across individual neurons. MIDAS can be used to simultaneously probe the individual genomes of many cells from patients with neurological diseases, and thus will allow identification of a range of structural genomic variants and eventually accurate determination of the influence of somatic CNVs on brain disorders in a high-throughput manner.

Recently, other single-cell sequencing methods that reduce amplification bias and increase genomic coverage have been reported. One such method utilizes a microfluidic device to isolate single cells and perform whole genome amplification in a 60-nl volume[10]. Another method, MALBAC, incorporates a novel enzymatic strategy to amplify single DNA molecules initially through quasi-linear amplification to a limited magnitude before exponential amplification and library construction[18]. MALBAC has been performed in microliter reactions in conventional reaction tubes. MIDAS represents an orthogonal strategy that adapts MDA to a microwell array. We compared data generated from single neurons amplified with MIDAS to previously published data from combined (and therefore diploid) pools of two single sperm cells amplified using standard in-tube MDA[32], the microfluidic device[10] and MALBAC[18,33]. To ensure a fair comparison, we normalized sequencing depth to an equal amount for each method and processed the raw sequencing data for each sample using an identical computational pipeline. We also compared MIDAS to a single SW480 cancer cell amplified by MALBAC. In this case, to ensure a fair comparison to the primarily diploid cell analyzed using MIDAS, we limited our analysis to regions consistently identified as diploid in the cancer cell (parts of chromosomes 1, 4, 6, 8, 10 and 15)[18]. MIDAS compares favorably to each amplification method (**Fig. 5** and **Supplementary Fig. 9**), generating the lowest levels of bias across the genome.

Several aspects of MIDAS could be improved. First, the current efficiency of amplification is limited to 10%, owing to the use of a low cell-loading density to avoid having more than one cell per microwell. This efficiency could be improved three to fivefold by increasing the cell loading density, imaging the microwell arrays containing fluorescently stained cells before amplification and excluding the wells with more than one cell from further analyses. Second, amplicon extraction by micromanipulation is currently performed manually at a speed of ~10 amplicons per hour. This number could be improved by at least one order of magnitude by implementing robotic automation. Third, the polydimethylsiloxane (PDMS) microwell arrays used for cell loading are highly customizable but require access to a microfabrication facility. Routine practice of MIDAS will depend on the commercial availability of hydrophilic microwell arrays. Finally, although each single cell is physically segregated into one microwell, the cells are not in total fluidic isolation. Thus, there may be the potential for cross-contamination between wells, and fluorescent imaging is required at least before and after MIDAS in order to ensure only single-cell amplicons are used.

MIDAS has the potential to provide researchers with a powerful tool for many other applications, including high-coverage, end-to-end haplotyping of mammalian genomes or probing *de novo* CNV events at the single-cell level during the induction of pluripotency or stem cell differentiation[34]. MIDAS allows for efficient high-throughput sequencing of a variety of organisms. This technology should help propel single-cell genomics, enhance our ability to identify diversity in multicellular organisms and lead to the discovery of a multitude of new organisms in various environments.

METHODS

Methods and any associated references are available in the online version of the paper.

Accession codes. SRA: SRP026348 and SRP026350.

Note: Any Supplementary Information and Source Data files are available in the online version of the paper.

ACKNOWLEDGMENTS

We thank C. Chen, H. Choi and the UCSD Nano3 facility for initial help with microwell fabrication, F. Liang for initial technical assistance and P. Pevzner for advice on *de novo* genome assembly. This project was funded by US National Institutes of Health grants R01HG004876, R01GM097253, U01MH098977 and P50HG005550, and National Science Foundation grant OCE-1046368.

AUTHOR CONTRIBUTIONS

J.G. and K.Z. conceived and designed the experiments. J.G., A.R. and H.-I.C. performed the experiments. J.G. and Y.-J.C. fabricated the microwell arrays. H.-L.F. performed sequencing. D.B. provided neuronal nuclei. J.G., A.G. and K.Z. analyzed data and wrote the manuscript with input from Y.-H.L. and J.C.

COMPETING FINANCIAL INTERESTS

The authors declare competing financial interests: details are available in the online version of the paper.

1. Zhang, K. *et al.* Sequencing genomes from single cells by polymerase cloning. *Nat. Biotechnol.* **24**, 680–686 (2006).
2. Rodrigue, S. *et al.* Whole genome amplification and *de novo* assembly of single bacterial cells. *PLoS ONE* **4**, e6864 (2009).
3. Fan, H.C., Wang, J., Potanina, A. & Quake, S.R. Whole-genome molecular haplotyping of single cells. *Nat. Biotechnol.* **29**, 51–57 (2011).
4. Hou, Y. *et al.* Single-cell exome sequencing and monoclonal evolution of a JAK2-negative myeloproliferative neoplasm. *Cell* **148**, 873–885 (2012).
5. Pan, X. *et al.* A procedure for highly specific, sensitive, and unbiased whole-genome amplification. *Proc. Natl. Acad. Sci. USA* **105**, 15499–15504 (2008).
6. Marcy, Y. *et al.* Dissecting biological "dark matter" with single-cell genetic analysis of rare and uncultivated TM7 microbes from the human mouth. *Proc. Natl. Acad. Sci. USA* **104**, 11889–11894 (2007).
7. Yoon, H.S. *et al.* Single-cell genomics reveals organismal interactions in uncultivated marine protists. *Science* **332**, 714–717 (2011).
8. Navin, N. *et al.* Tumour evolution inferred by single-cell sequencing. *Nature* **472**, 90–94 (2011).
9. Xu, X. *et al.* Single-cell exome sequencing reveals single-nucleotide mutation characteristics of a kidney tumor. *Cell* **148**, 886–895 (2012).

10. Wang, J., Fan, H.C., Behr, B. & Quake, S.R. Genome-wide single-cell analysis of recombination activity and *de novo* mutation rates in human sperm. *Cell* **150**, 402–412 (2012).
11. Bankevich, A. *et al.* SPAdes: a new genome assembly algorithm and its applications to single-cell sequencing. *J. Comput. Biol.* **19**, 455–477 (2012).
12. Chitsaz, H. *et al.* Efficient *de novo* assembly of single-cell bacterial genomes from short-read data sets. *Nat. Biotechnol.* **29**, 915–921 (2011).
13. Hutchison, C.A. III, Smith, H.O., Pfannkoch, C. & Venter, J.C. Cell-free cloning using phi29 DNA polymerase. *Proc. Natl. Acad. Sci. USA* **102**, 17332–17336 (2005).
14. Marcy, Y. *et al.* Nanoliter reactors improve multiple displacement amplification of genomes from single cells. *PLoS Genet.* **3**, 1702–1708 (2007).
15. Inoue, J., Shigemori, Y. & Mikawa, T. Improvements of rolling circle amplification (RCA) efficiency and accuracy using Thermus thermophilus SSB mutant protein. *Nucleic Acids Res.* **34**, e69 (2006).
16. Woyke, T. *et al.* One bacterial cell, one complete genome. *PLoS ONE* **5**, e10314 (2010).
17. Fitzsimons, M.S. *et al.* Nearly finished genomes produced using gel microdroplet culturing reveal substantial intraspecies genomic diversity within the human microbiome. *Genome Res.* **23**, 878–888 (2013).
18. Zong, C., Lu, S., Chapman, A.R. & Xie, X.S. Genome-wide detection of single-nucleotide and copy-number variations of a single human cell. *Science* **338**, 1622–1626 (2012).
19. Blainey, P.C. & Quake, S.R. Digital MDA for enumeration of total nucleic acid contamination. *Nucleic Acids Res.* **39**, e19 (2011).
20. Adey, A. & Shendure, J. Ultra-low-input, tagmentation-based whole-genome bisulfite sequencing. *Genome Res.* **22**, 1139–1143 (2012).
21. Rehen, S.K. *et al.* Constitutional aneuploidy in the normal human brain. *J. Neurosci.* **25**, 2176–2180 (2005).
22. Rehen, S.K. *et al.* Chromosomal variation in neurons of the developing and adult mammalian nervous system. *Proc. Natl. Acad. Sci. USA* **98**, 13361–13366 (2001).
23. Yang, A.H. *et al.* Chromosome segregation defects contribute to aneuploidy in normal neural progenitor cells. *J. Neurosci.* **23**, 10454–10462 (2003).
24. Yurov, Y.B. *et al.* Aneuploidy and confined chromosomal mosaicism in the developing human brain. *PLoS ONE* **2**, e558 (2007).
25. Muotri, A.R. & Gage, F.H. Generation of neuronal variability and complexity. *Nature* **441**, 1087–1093 (2006).
26. Singer, T., McConnell, M.J., Marchetto, M.C., Coufal, N.G. & Gage, F.H. LINE-1 retrotransposons: mediators of somatic variation in neuronal genomes? *Trends Neurosci.* **33**, 345–354 (2010).
27. Westra, J.W. *et al.* Neuronal DNA content variation (DCV) with regional and individual differences in the human brain. *J. Comp. Neurol.* **518**, 3981–4000 (2010).
28. Baslan, T. *et al.* Genome-wide copy number analysis of single cells. *Nat. Protoc.* **7**, 1024–1041 (2012).
29. Shendure, J. *et al.* Accurate multiplex polony sequencing of an evolved bacterial genome. *Science* **309**, 1728–1732 (2005).
30. Abecasis, G.R. *et al.* An integrated map of genetic variation from 1,092 human genomes. *Nature* **491**, 56–65 (2012).
31. Albertsen, M. *et al.* Genome sequences of rare, uncultured bacteria obtained by differential coverage binning of multiple metagenomes. *Nat. Biotechnol.* **31**, 533–538 (2013).
32. Kirkness, E.F. *et al.* Sequencing of isolated sperm cells for direct haplotyping of a human genome. *Genome Res.* **23**, 826–832 (2013).
33. Lu, S. *et al.* Probing meiotic recombination and aneuploidy of single sperm cells by whole-genome sequencing. *Science* **338**, 1627–1630 (2012).
34. Hussein, S.M. *et al.* Copy number variation and selection during reprogramming to pluripotency. *Nature* **471**, 58–62 (2011).
35. Westra, J.W. *et al.* Aneuploid mosaicism in the developing and adult cerebellar cortex. *J. Comp. Neurol.* **507**, 1944–1951 (2008).
36. Huson, D.H., Auch, A.F., Qi, J. & Schuster, S.C. MEGAN analysis of metagenomic data. *Genome Res.* **17**, 377–386 (2007).

ONLINE METHODS

Microwell array fabrication. Microwell arrays were fabricated from PDMS. Each array was 7 mm × 7 mm, with two rows of eight arrays per slide and 255 microwells per array. The individual microwells were 400 µm in diameter and 100 µm deep (~12 Nl volume), and were arranged in honeycomb patterns in order to minimize space in between the wells. To fabricate the arrays, first, we created an SU-8 mold using soft lithography at the Nano3 facility at UC San Diego. Next, a 10:1 ratio of polymer to curing agent mixture of PDMS was poured over the mold. Finally, the PDMS was degassed and cured for 3 h at 65 °C.

Bacteria and neuron preparation. *E. coli* K12 MG1655 was cultured overnight, collected in log-phase and washed 3× in PBS. After quantification, the solution was diluted to 10 cells/µl. Human neuronal nuclei were isolated as previously described[27,35] and fixed in ice-cold 70% ethanol. Nuclei were labeled with a monoclonal mouse antibody against NeuN (1:100 dilution) (Chemicon, Temecula, CA) and an Alexa Fluor 488 goat anti-mouse IgG secondary antibody (1:500 dilution) (Life Technologies, San Diego, CA). Nuclei were counterstained with propidium iodide (50 µg/ml) (Sigma, St. Louis, MO) in PBS solution containing 50 µg/ml RNase A (Sigma) and chick erythrocyte nuclei (Biosure, Grass Valley, CA). Nuclei in the G1/G0 cell cycle peak, determined by propidium iodide fluorescence, were electronically gated on a Becton Dickinson FACS Aria II (BD Biosciences, San Jose, CA) and selectively collected based on NeuN$^+$ immunoreactivity.

Cell seeding, lysis and MDA. All reagents not containing DNA or enzymes were first exposed to ultraviolet light for 10 min before use. The PDMS slides were treated with oxygen plasma to make them hydrophilic and ensure random cell seeding. The slides were then treated with 1% bovine serum albumin (BSA) (EMD Chemicals, Billerica, MA) in phosphate-buffered saline (PBS) (Gibco, Grand Island, NY) for 30 min and washed 3× with PBS to prevent DNA from sticking to the PDMS. The slides were completely dried in a vacuum before cell seeding. Cells were diluted in 1× PBS to a concentration of 0.1 cells per well per array, and 3 µL of cell dilution was added to each array. This dilution ensures that ~99.5% of the wells have no more than one cell.

Initially, to verify that cell seeding adhered to the Poisson distribution, cells were stained with 1× SYBR green and viewed under a fluorescent microscope. Proper cell distribution was further confirmed with s.e.m. imaging. For s.e.m. imaging, chromium was sputtered onto the seeded cells for 6 s to increase conductivity. Note that the imaging of cell seeding was used only to confirm the theoretical Poisson distribution and not performed during actual amplification and sequencing experiments due to the potential introduction of contamination.

After seeding, cells were left to settle into the wells for 10 min. The seeded cells were then lysed either with 300 U ReadyLyse lysozyme at 100 U/µl (Epicentre, Madison, WI) and incubation at room temperature for 10 min, or with five 1-min freeze/thaw cycles using a dry ice brick and room temperature in a laminar flow hood. After lysis, 4.5 µl of alkaline lysis (ALS) buffer (400 mM KOH, 100 mM DTT, 10 mM EDTA) was added to each array and incubated on ice for 10 min. Then, 4.5 µl of neutralizing (NS) buffer (666 mM Tris-HCl, 250 mM HCL) was added to each array. 11.2 µl of MDA master mix (1× buffer, 0.2× SYBR green I, 1 mM dNTP's, 50 µM thiolated random hexamer primer, 8U phi29 polymerase, Epicentre, Madison, WI) was added and the arrays were then covered with mineral oil. The slides were then transferred to the microscope stage enclosed in a custom temperature controlled incubator set to 30 °C. Images were taken at 30-min intervals for 10 h using a 488-nm filter.

Image analysis. Images were analyzed with a custom Matlab script to subtract background fluorescence. Because SYBR Green I was added to the MDA master mix, fluorescence under a 488-nm filter was expected to increase over time for positive amplifications. If a digital profile of fluorescent wells with increasing fluorescence over time was observed (~10–20 wells per array), the array was kept. If no wells fluoresced, amplification failed and further experiments were stopped. Alternatively, if a majority of the wells fluoresced, the array was considered to have exogenous contamination from environmental DNA and subsequent analysis was similarly stopped. If two abutting wells fluoresced, neither was extracted due to the higher likelihood of more than one cell in each well existing (as in this case, seeding was potentially nonuniform). Finally, only wells with amplicons originating from a single point were extracted, ensuring that only single cell–derived amplicons were processed; thus, any potential cross-well contamination was prevented.

Amplicon extraction. 1 mm outer diameter glass pipettes (Sutter, Novato, CA) were pulled to ~30 µm diameters, bent to a 45 degree angle under heat, coated with SigmaCote (Sigma, St. Louis, MO) and washed three times with dH$_2$0. Wells with positive amplification were identified using the custom Matlab script described above. A digital micromanipulation system (Sutter, Novato, CA) was used for amplicon extraction. The glass pipette was loaded into the micromanipulator and moved over the well of interest. The microscope filter was switched to bright field and the pipette was lowered into the well. Negative pressure was slowly applied, and the well contents were visualized proceeding into the pipette. The filter was then switched back to 488 nm to ensure the well no longer contained any fluorescent material. Amplicons were deposited in 1 µl dH$_2$0.

Amplicon quantification. For quantification of microwell amplification, 0.5 µl of amplicon was amplified a second time using MDA in a 20-µl PCR tube reaction (1× buffer, 0.2× SYBR green I, 1 mM dNTPs, 50 mM thiolated random hexamer primer, 8U phi29 polymerase). After purification using Ampure XP beads (Beckman Coulter, Brea, CA), the second round amplicon was quantified using a Nanodrop spectrophotometer. The second round amplicon was then diluted to 1 ng, 100 pg, 10 pg, 1 pg and 100 fg to create an amplicon ladder. Subsequently, the remaining 0.5 µl of the first round amplicon was amplified using MDA along with the amplicon ladder in a quantitative PCR machine. The samples were allowed to amplify to completion, and the time required for each to reach 0.5× of the maximum fluorescence was extracted. The original amplicon concentration could then be interpolated. This second round of MDA was only performed during amplicon quantification in order to determine approximately how much DNA was produced in each microwell. Amplicons that were sequenced were only subjected to the initial round of MDA, and thus did not have any secondary MDA or quantification performed.

Low-input library construction. 1.5 µl of ALS buffer was added to the extracted amplicons to denature the DNA followed by a 3-min incubation at room temperature. 1.5 µl of NS buffer was added on ice to neutralize the solution. 10 U of DNA polymerase I (Invitrogen, Carlsbad, CA) was added to the denatured amplicons along with 250 nanograms of unmodified random hexamer primer, 1 mM dNTPs, 1× Ampligase buffer (Epicentre, Madison, Wi) and 1× NEB buffer 2 (NEB, Cambridge, MA). The solution was incubated at 37 °C for 1 h, allowing second strand synthesis. 1 U of Ampligase was added to seal nicks and the reaction was incubated first at 37 °C for 10 min and then at 65 °C for 10 min. The reaction was cleaned using standard ethanol precipitation and eluted in 4 µl water.

Nextera transposase enzymes (Epicentre, Madison, WI) were diluted 100-fold in 1× TE buffer and glycerol. 10 µL transposase reactions were then conducted on the eluted amplicons after addition of 1 µL of the diluted enzymes and 1× tagment DNA buffer. The reactions were incubated for 5 min at 55 °C for mammalian cells and 1 min at 55 °C for bacterial cells. 0.05 U of protease (Qiagen, Hilden, Germany) was added to each sample to inactivate the transposase enzymes; the protease reactions were incubated at 50 °C for 10 min followed by 65 °C for 20 min. 5 U Exo minus Klenow (Epicentre, Madison, WI) and 1 mM dNTPs were added and incubated at 37 °C for 15 min followed by 65 °C for 20 min. Two-stage quantitative PCR using 1× KAPA Robust 2G master mix (Kapa Biosystems, Woburn, MA), 10 µM Adaptor 1, 10 µM barcoded Adaptor 2 in the first stage, and 1× KAPA Robust 2G master mix, 10 µM Illumina primer 1, 10 µM Illumina primer 2 and 0.4× SYBR Green I in the second stage was performed and the reaction was stopped before amplification curves reached their plateaus. The reactions were then cleaned up using Ampure XP beads in a 1:1 ratio. A 6% PAGE gel verified successful tagmentation reactions.

Bulk sample library construction. Genomic DNA was extracted from ~4,000 neuronal nuclei using the DNeasy blood and tissue kit (Qiagen, Hilden,

doi:10.1038/nbt.2720

Germany). The genomic DNA was incubated with 1 µl undiluted Nextera transposase enzymes and 1× tagment DNA buffer for 5 min at 55 °C. The reactions were cleaned with MinElute columns (Qiagen, Hilden, Germany) and eluted in 20 µl water. 5 U Exo minus Klenow (Epicentre, Madison, WI) and 1 mM dNTPs were added and incubated at 37 °C for 15 min followed by 65 °C for 20 min. Two-stage quantitative PCR using 1× KAPA Robust 2G master mix (Kapa Biosystems, Woburn, MA), 10 µM Adaptor 1, 10 µM barcoded Adaptor 2 in the first stage, and 1× KAPA Robust 2G master mix, 10 µM Illumina primer 1, 10 µM Illumina primer 2 and 0.4× SYBR Green I in the second stage was performed and the reaction was stopped before amplification curves reached their plateaus. The reactions were then cleaned up using Ampure XP beads in a 1:1 ratio. A 6% PAGE gel verified successful tagmentation reactions.

Mapping and *de novo* assembly of bacterial genomes. Bacterial libraries were selected into the 300- to 600-bp range and sequenced in an Illumina MiSeq using 100-bp paired-end reads. *E. coli* data were mapped both to the reference genome and the *de novo* assembled. For the mapping analysis, libraries were mapped as single-end reads to the reference *E. coli* K12 MG1655 genome using default Bowtie parameters with removal of any reads with multiple matches. Contamination was analyzed, and clonal reads were removed using SAMtools' rmdup function. Chimeras were analyzed by flagging paired reads on the same strand or paired reads with a mismatched orientation. Chimeric junctions were defined as the number of chimeric reads divided by the total number of mapped bases. For the *de novo* assembly, paired end reads with a combined length less than 200 bp were first joined and treated as single-end reads. All remaining paired-end reads and newly generated single-end reads were then quality trimmed. *De novo* assembly was performed using SPAdes[11] v. 2.4.0. Corrected reads were assembled with k-mer values of 21, 33 and 55. The assembled scaffolds were mapped to the NCBI nt database with BLAST, and the organism distribution was visualized using MEGAN[36]. Obvious contaminants (e.g., human) were removed from the assembly and the assembly was analyzed using QUAST[37]. The remaining contigs were annotated using RAST[38] and KAAS[39].

Identification of CNVs in MIDAS and MDA data. Mammalian single-cell libraries were sequenced in an Illumina Genome Analyzer II× or Illumina HiSeq using 36-bp single-end reads. The CNV algorithm previously published by Cold Spring Harbor Laboratories[8] was used to call CNV on each single neuron, with modifications to successfully analyze non-cancer cells. Briefly, for each sample, reads were mapped to the genome using Bowtie. Clonal reads resulting from PCR artifacts were removed using SAMtools, and the remaining unique reads were then assigned into 49,891 genomic bins of ~60 kb in size that were previously determined such that each would contain a similar number of reads after mapping[28]. Each bin's read count was then expressed as a value relative to the average number of reads per bin in the sample, and then normalized by GC content of each bin using a weighted sum of least-squares algorithm (LOWESS). Circular binary segmentation was then used to divide each chromosome's bins into adjacent segments with similar means. Unlike the previously published algorithm, in which a histogram of bin counts was then plotted and the second peak chosen as representing a copy number of two, it was assumed, owing to samples not being cancerous and thus being unlikely to contain significant amounts of aneuploidy, that the mean bin count in each sample would correspond to a copy number of two. Each segment's normalized bin count was thus multiplied by two and rounded to the nearest integer to call copy number. MIDAS data clearly showed a CNV call designating trisomy 21 in all Down syndrome single cells, whereas the traditional MDA-based method was not able to call trisomy 21.

Identification of artificial CNVs in MDA and MIDAS data. To test the ability of the CNV algorithm described above to call small CNVs, we constructed artificial CNVs computationally. Prior to circular binary segmentation, in each Down syndrome sample, 100 random genomic regions across chromosomes 1–22 were chosen, each consisting of either 17 or 34 bins of ~60 kb in size. Each region was replaced with an equivalently sized region from chromosome 21 or chromosome 4 (**Supplementary Table 5**). The above algorithm was then run on each 'spiked-in' sample, and the number of new CNV calls in each sample that matched each spike-in was tallied. For the chromosome 21 spike-ins, MIDAS was able to accurately call 98% of spiked-in CNVs at the 2-Mb level and 68% of spiked-in CNVs at the 1-Mb level, whereas the traditional MDA-based method was not able to call any spiked-in CNVs. As expected, spike-ins of chromosome 4 did not result in any additional CNV calls.

37. Gurevich, A., Saveliev, V., Vyahhi, N. & Tesler, G. QUAST: quality assessment tool for genome assemblies. *Bioinformatics* **29**, 1072–1075 (2013).
38. Aziz, R.K. *et al.* The RAST Server: rapid annotations using subsystems technology. *BMC Genomics* **9**, 75 (2008).
39. Moriya, Y., Itoh, M., Okuda, S., Yoshizawa, A.C. & Kanehisa, M. KAAS: an automatic genome annotation and pathway reconstruction server. *Nucleic Acids Res.* **35**, W182–W185 (2007).

doi:10.1038/nbt.2720